Nanostructures

DOI: 10.1002/anie.200701307

Tetrahedral Colloidal Crystals of Ag_2S Nanocrystals**

Zhongbin Zhuang, Qing Peng, Xun Wang, and Yadong Li**

Monodisperse nanocrystals,[1–3] as ideal building blocks, can be used to fabricate superlattice assemblies of ordered particles through "bottom-up" assembly. The as-obtained superlattice assemblies raise the possibility of combining the properties of individual nanocrystals with new bulk physical properties.[4–14] On the other hand, monodisperse nanocrystals can also be considered as "artificial atoms", as they exhibit similar behaviors to atoms and/or ions.[1–3,14,15] The nanoparticle units are large enough to be directly observed under an electron microscope; thus, the nanoparticle crystals are good models for investigation by crystallography, which is the guideline for nanocrystal growth.[16,17] Owing to these significant properties and potential in fundamental research, nanocrystals have gained more and more attention for their use in simply and conveniently fabricating highly ordered superlattice assemblies.[4–14] The pioneer work of Bawendi and co-workers has provided a bottom-up assembly approach to construct 3D superlattices by using CdSe quantum dots as building blocks.[4] More recently, Grzybowski and co-workers successfully developed the electrostatic self-assembly (ESA) method for fabricating Au/Ag nanoparticle crystals with a diamond-like lattice.[14] The processes in all of these examples must precisely control the composition, size, shape, and surface chemistry of the nanocrystal building blocks first, and subsequently assemble them through a physical process. These methods provide a general route; however, the complexity of the process has confined the development of research in superlattice assemblies.

Herein, we report a simple one-step, two-phase reaction to assemble Ag_2S nanocrystals into tetrahedral colloidal aggregates comprising of a perfectly ordered 3D superlattice structure. Dodecanethiol was chosen as both the sulfur source and the structure-directing agent. A plausible mechanism has been proposed that consists of self-assembly, breaking, and layer-by-layer stacking. Because the Ag_2S colloidal crystals are capped with a hydrophobic layer of dodecanethiol, the Ag_2S colloidal aggregates consisting of superlattices can be well-dispersed in a nonpolar solvent, in which they grow further. This result indicates that nanocrystals may serve as building blocks for constructing integrated macroscopic devices. Thus, the artificial atoms (that is, the nanocrystals) and their superlattices can provide a good model for direct investigation of the crystal growth.

The dynamic light scattering (DLS) spectrum (Supporting Information, Figure S1) shows that the Ag_2S nanocrystals form aggregates in solution. Surprisingly, TEM and SEM images show that the special Ag_2S nanocrystals form very ordered arrays in the aggregates. It can be seen that the aggregates have a triangular shape in the 2D projection direction, and the edge length of the triangle is about 100–1000 nm (Figure 1a). Clearly, the magnified TEM image

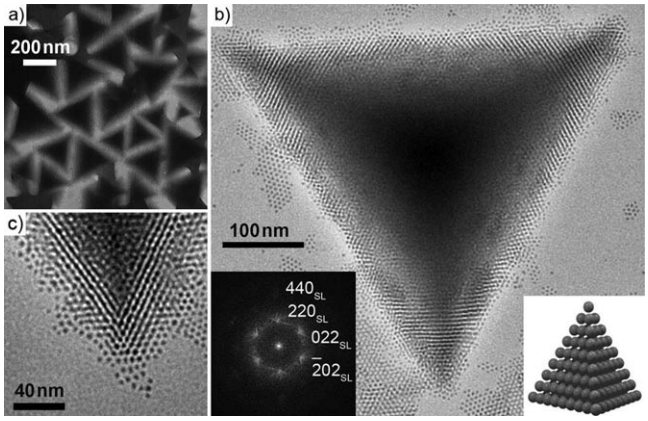

Figure 1. TEM images of the obtained Ag_2S tetrahedral superlattice colloidal crystals. a) TEM image at low magnification; b) a typical TEM image of an individual tetrahedron at high magnification; the left inset is the FFT pattern of the superlattice and the right inset is a scheme of the tetrahedral superlattice colloidal crystal; c) a magnified TEM image of a vertex of the tetrahedron.

(Figure 1b) of an individual triangle illustrates that the contrast becomes gradually sharper from the edge to the center, and it is too dark to show any details near the center domain. This observation indicates that the samples have 3D structures with tetrahedral shape, which are proved by the 3D stereoscopic effect shown in the SEM image (Supporting Information, Figure S2). The 3D nature was further confirmed by TEM rotation experiments (Supporting Information, Figure S3). The movement of the dark domain when the specimen is rotated confirms that the sample is a true 3D structure (regular tetrahedron), instead of a quasi-2D triangular plate.

By careful investigation of Figure 1b,c (magnified TEM image of a vertex of the tetrahedron), it can be found that the tetrahedra are built up of uniform nanocrystals. The nanocrystals have an average diameter of about 3.5 ± 0.5 nm and form a highly ordered close-packed 3D superlattice structure. The fast Fourier transform (FFT) pattern displays the highly

[*] Z. Zhuang, Dr. Q. Peng, Dr. X. Wang, Prof. Y. Li
Department of Chemistry, Tsinghua University
Beijing, 100084 (China)
Fax: (+86) 10-6278-8765
E-mail: pengqing@mail.tsinghua.edu.cn
ydli@mail.tsinghua.edu.cn

[**] This work was supported by NSFC (20401010, 50372030, 90606006) and the State Key Project of Fundamental Research (2006CB932301, 2006CB932303, 2006CB932608).

Supporting information for this article is available on the WWW under http://www.angewandte.org or from the author.

ordered stacking of the building blocks (the left inset of Figure 1b). The interparticle spacing of the nanocrystals is about 2 nm, which is consistent with the effective thickness of dodecanethiol.[7] The tetrahedral colloidal supercrystals have well-defined edges and sharp vertices composed of only a few of nanocrystals (Figure 1c). The right inset of Figure 1b shows a scheme of the tetrahedral colloidal crystal superlattice.

The symmetry and structure of the superlattice tetrahedron were studied by small-angle X-ray diffraction (SAXRD; Figure 2a). The five peaks correspond to *d* spacings of 45, 39, 23, 22, and 20 Å. These peaks display *d*-value ratios of $\sqrt{3}:\sqrt{4}:\sqrt{11}:\sqrt{12}:\sqrt{16}$, which can be indexed as (111), (200), (311), (222), and (400) reflections, respectively, in the face-centered-cubic superlattices with $a = 7.8$ nm. On the basis of the discussion in the literature,[18] small Ag_2S nanocrystals (less than 5 nm) can be obtained by the decomposition of silver alkylthiolates at high temperature (greater than 220 °C). The wide-angle XRD pattern (solid curve shown in Figure 2b) shows several broad peaks because of the small sizes of these nanocrystals. However, the nanocrystals can not be indexed to Ag_2S since the peaks are dramatically broadened. On the basis of the standard Ag_2S diffraction patterns (JCPDF Card No. 24-0715), we simulated the diffraction peaks of 3.5-nm Ag_2S nanocrystals by using a Gaussian distribution, and the peak width at half-height was calculated by the Scherrer equation (the dashed line shown in Figure 2b). This simulation is almost consistent with our experimental data and confirms that the product was small Ag_2S nanocrystals. In addition, after the as-prepared sample are annealed for 1 h at 300 °C in air, the XRD patterns show that the treated sample is Ag_2S (Supporting Information, Figure S4). Furthermore, the energy-dispersive X-ray analysis (EDAX) results show the element signals of C, S, and Ag (Supporting Information, Figure S5), which confirms that the nanocrystals are Ag_2S capped by dodecanethiol.

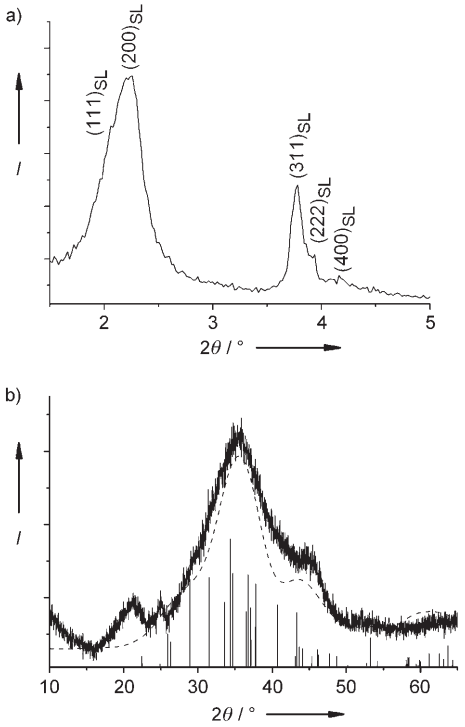

Figure 2. a) Small-angle XRD pattern; b) wide-angle XRD pattern of the tetrahedral colloidal crystals; solid curve: experimental result; dashed line: simulated result; vertical line: standard reflections (JCPDF Card No. 24-0715).

On the basis of previous studies, when the volume fraction of spheres is increased to 55%, monodisperse hard spheres dispersed in the solution will spontaneously assemble into ordered arrays because of the increase in entropy.[7,11] The local free space for each nanocrystal is larger in the ordered structure than that in the disordered structure. Furthermore, the interactions (van der Waals attraction) between the dodecanethiol molecules capped on the Ag_2S nanocrystals lead to low energy in the superlattice system. Different crystallographic planes usually have different surface energies. The surface energy of the {111} plane is lower than those of the {100} and {110} planes.[19] The tetrahedron has the minimal surface energy owing to the four $\{111\}_{SL}$ equivalent faces (SL = superlattice).

However, there are still some 2D superlattice flakes in our prepared samples. They are considered as intermediate products that may play important roles in the formation of 3D ordered colloidal crystals. Based on our experimental results, it seems that the tetrahedral structure is constructed layer-by-layer by a series of quasi-2D superlattice triangular flakes. Figure 3 shows a schematic representation of a plausible formation mechanism for tetrahedral colloidal crystals. A two-phase reaction system has been designed to control the synthesis and assembly of the nanocrystals. In our reaction system, the Ag source ($[Ag(NH_3)_2]^+$) is in the aqueous phase, while the upper oil phase (dodecanethiol) provides the sulfur source. First, a phase-transfer process occurs, in which $[Ag(NH_3)_2]^+$ in aqueous solution reacts with dodecanethiol at the water–oil interfaces to form a silver dodecanethiol complex (step a). At 200 °C, the complex decomposes and forms Ag_2S nanocrystals capped by excess dodecanethiol (step b). This process suppresses the further growth of nanocrystals and gives the nanocrystals a hydro-

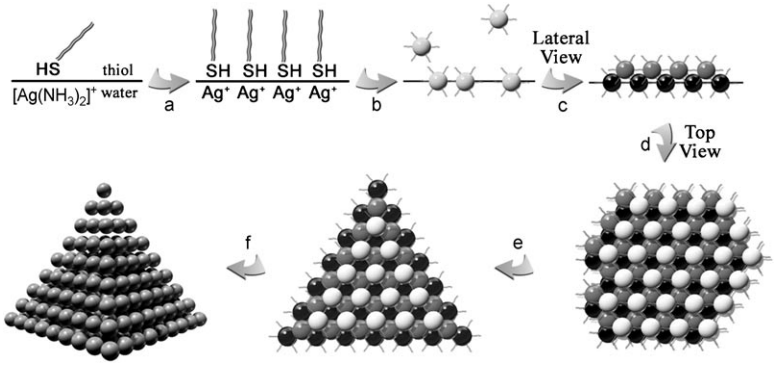

Figure 3. A schematic illustration of the plausible formation mechanism of the tetrahedral superlattice colloidal crystals; steps a–f are explained in the text.

phobic shell. For the as-capped nanocrystals, dodecanethiol is a good solvent, but water is a nonsolvent. These nanocrystals self-assemble at the interface of water and dodecanethiol (step c).[10] Several nanocrystals pack together into 2D cubic-close-packed superlattice flakes (the intermediate product; step d). When the superlattice flakes grow large enough, they break along the lowest-energy $\{111\}_{SL}$ face to form triangle-shaped superlattices (step e). The free nanocrystals in the solution stack over the triangle substrate layer-by-layer to form a 3D superlattice, and finally generate a tetrahedral colloidal crystal to further reduce the surface energy (step f).

The TEM image in Figure 4a shows these intermediates. These irregular superlattice flakes have a tendency to break along the $\{111\}_{SL}$ face (pointed out by solid arrows). Meanwhile, some nearly triangular flakes appear (pointed out by hollow arrows). A magnified TEM image of an individual triangular flake is shown in Figure 4b; these triangles are bases for tetrahedra. In Figure 4a, it can be seen that a few of the integrated tetrahedra have been assembled among the flakes. The magnified TEM images of irregular flakes (Figure S6 in the Supporting Information) show that they are constructed by nanocrystals in ordered arrays.

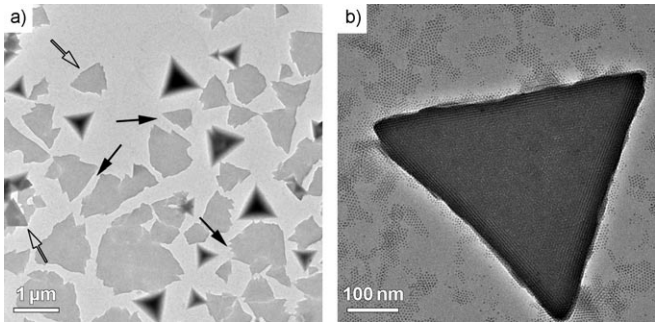

Figure 4. TEM images of the intermediate products. a) Mixture of primary generated superlattice flakes and final tetrahedra; the solid and hollow arrows are explained in the text; b) a magnified image of a typical triangular flake.

Nanocrystals are often called "artificial atoms", as they have similar properties to atoms and/or ions.[1–3,14,15] They are large enough that they can be clearly observed by electron microscopy, but not too large to be stable in solution. Thus, the superlattice provides a good model for direct investigation of the behavior of crystals and free units, and it may be useful in nanocrystal growth.[16,17] Based on our calculations, each superlattice tetrahedron in our experiments contains about 10^5 nanocrystals, which is similar to the amount of atoms in a nanocrystal.[4] Thus, we think that our obtained tetrahedral superlattice crystals may be a good choice for investigating crystallization. Like the behavior of a traditional crystal, these tetrahedral colloidal crystals may grow or dissolve in solution (and hold the superlattice structure during the process), and finally the free nanocrystals and the colloidal crystals achieve a dynamic equilibrium. By slow evaporation of the solvent, the colloidal crystals can be built up gradually. The final size is up to several micrometers (Figure 5a). During the growth process, a series of interesting new morphologies have been observed. Four small tetrahedra can combine through their $\{111\}_{SL}$ face and form a "twinned" structure (Figure 5b and Figure S7a,b in the Supporting Information), with the symmetry increasing from T_d to O_h. Upon evaporating and condensing for a long time, a number of small tetrahedra can also aggregate into a larger, more complex colloidal crystal. This kind of colloidal crystal looks like many small tetrahedron hills standing on a plane, and the whole body still has a large tetrahedral shape (Figure 5c and Figure S7c,d in the Supporting Information). The inset FFT pattern in Figure 5c indicates that the whole nanoparticle crystal remains a single supercrystal. However, upon introducing more cyclohexane into the system, the tetrahedron can redissolve and finally decompose to free nanocrystals dispersed in the solution. The vertices of the tetrahedron contain only a few nanocrystals, and the interactions are weak in these areas. Thus, the nanocrystals at the vertices are not as tightly bound, and a truncated tetrahedron is generated first (Figure 5d). If a large

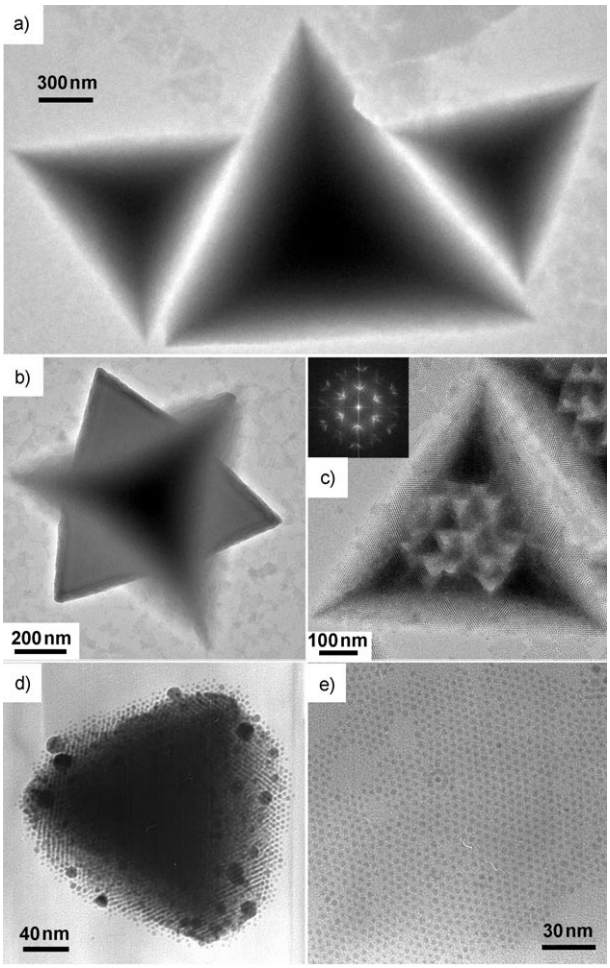

Figure 5. Different morphologies of the superlattice colloidal crystals. a) TEM image of some extra-large tetrahedral superlattice colloidal crystals obtained by slowly evaporating the solvent for several days; the edges of the tetrahedra are up to 1 μm; b) TEM image of "twin" tetrahedra; c) TEM image of a typical aggregated tetrahedral superlattice colloidal crystal; the inset is the FFT pattern, which indicates that the whole superlattice crystal has the same lattice; d) TEM image of a nearly spherical colloidal crystal; the vertices of the tetrahedral colloidal crystals have been dissolved first; e) TEM image of the totally redissolved colloidal crystals, which are nearly monodisperse nanocrystals.

amount of cyclohexane is added into the solvent, the tetrahedral colloidal crystals redissolve completely into free-standing nanocrystals (Figure 5e).

In this work, a similar process in which superlattice colloidal crystals are synthesized and assembled directly from $[Cu(NH_3)_4]^{2+}$ and dodecanethiol (Supporting Information, Figure S8) was developed. This two-phase synthetic method may be extended to the direct synthesis of other metal sulfide superlattice colloidal crystals.

In conclusion, faceted tetrahedral superlattice colloidal crystals have been directly prepared through a one-step, two-phase reaction without the presynthesis of uniform nanocrystals. The superlattice crystals exhibit four $\{111\}_{SL}$ equivalent faces and a tetrahedral shape. A plausible mechanism has been proposed that includes self-assembly, breaking, and layer-by-layer stacking. The "grow-and-dissolve" behavior exhibited in solution is similar to that of a true single crystal. This system provides a model that allows the investigation of crystals by using conventional instruments. This kind of tetrahedral colloidal crystals may serve as mesoscale building blocks for constructing integrated macroscopic architectures or devices for fundamental studies and future applications.

Experimental Section

In a typical procedure, $AgNO_3$ (0.85 g, 0.005 M) was dissolved in deionized water (20 mL) to form a clear solution. Ammonia was then introduced into the solution under agitation until all the generated dark precipitation disappeared. After continuous stirring for 15 min, the solution was transferred into a teflon-lined autoclave of 40-mL capacity, and dodecanethiol (3 mL) was added to the solution. The autoclave was sealed and heated at 200 °C for 5 h. After the reaction was cooled to room temperature, the product was collected, and the water remaining in the autoclave was discarded. Then, ethanol (20 mL) was introduced, and the product precipitated. The mixture was placed in a centrifuge for 5 min at 4800 rpm, and the precipitate was collected. It was redispersed in cyclohexane (10 mL) and centrifuged for 2 min at 4000 rpm; the supernatant was saved and any precipitates were discarded.

The structure and size of the superlattice colloidal crystals were measured by using transmission electron microscopy (TEM, JEOL JEM 1200EX working at 100 kV and FEI Tecnai G2 F20 S-Twin working at 200 kV). Samples were prepared by placing a drop of a dilute cyclohexane dispersion of product on the surface of a copper grid. Scanning electron microscopy (SEM, FEI Sirion 200 working at 10 kV) was also employed, and the sample was prepared by placing a drop of the dispersion on a silicon substrate. Energy-dispersive X-ray analysis (EDAX) of the product was also performed on the samples during the SEM measurements. The phase and superlattice structures were determined by XRD on a Bruker D8 Advance X-ray powder diffractometer with $Cu_{K\alpha}$ radiation ($\lambda = 1.5418$ Å). The sample was prepared by adding the dispersions dropwise onto a silicon wafer several times and drying under infrared lamp irradiation. The size distributions of the tetrahedral colloidal crystals dispersed in cyclohexane were determined by dynamic light scattering (DLS, Zetasiezer 3000HS) spectra.

Received: March 25, 2007
Revised: June 26, 2007
Published online: September 20, 2007

Keywords: interfaces · nanostructures · self-assembly · silver sulfide · superlattices

[1] a) C. B. Murray, D. J. Norris, M. G. Bawendi, *J. Am. Chem. Soc.* **1993**, *115*, 8706–8715; b) A. P. Alivisatos, *Science* **1996**, *271*, 933–937; c) X. G. Peng, L. Manna, W. D. Yang, J. Wickham, E. Scher, A. Kadavanich, A. P. Alivisatos, *Nature* **2000**, *404*, 59–61.
[2] X. Wang, J. Zhuang, Q. Peng, Y. D. Li, *Nature* **2005**, *437*, 121–124.
[3] Y. Yin, A. P. Alivisatos, *Nature* **2005**, *437*, 664–670.
[4] C. B. Murray, C. R. Kagan, M. G. Bawendi, *Science* **1995**, *270*, 1335–1338.
[5] a) P. V. Braun, P. Osenar, S. I. Stupp, *Nature* **1996**, *380*, 325–328; b) L. Motte, F. Billoudet, E. Lacaze, M. P. Pileni, *Adv. Mater.* **1996**, *8*, 1018–1020; c) C. J. Kiely, J. Fink, M. Brust, D. Bethell, D. J. Schiffrin, *Nature* **1998**, *396*, 444–446; d) A. K. Boal, F. Ilhan, J. E. DeRouchey, T. Thurn-Albrecht, T. P. Russell, V. M. Rotello, *Nature* **2000**, *404*, 746–748; e) M. M. Maye, S. C. Chun, L. Han, D. Rabinovich, C. J. Zhong, *J. Am. Chem. Soc.* **2002**, *124*, 4958–4959; f) F. Gao, Q. Y. Lu, D. Y. Zhao, *Nano Lett.* **2003**, *3*, 85–88; g) Y. Yang, S. M. Liu, K. Kimura, *Angew. Chem.* **2006**, *118*, 5790–5793; *Angew. Chem. Int. Ed.* **2006**, *45*, 5662–5665.
[6] a) C. A. Mirkin, R. L. Letsinger, R. C. Mucic, J. J. Storhoff, *Nature* **1996**, *382*, 607–609; b) W. Shenton, D. Pum, U. B. Sleytr, S. Mann, *Nature* **1997**, *389*, 585–587; c) M. Li, H. Schnablegger, S. Mann, *Nature* **1999**, *402*, 393–395.
[7] B. A. Korgel, S. Fullam, S. Connolly, D. Fitzmaurice, *J. Phys. Chem. B* **1998**, *102*, 8379–8388.
[8] a) S. H. Sun, C. B. Murray, D. Weller, L. Folks, A. Moser, *Science* **2000**, *287*, 1989–1992; b) C. T. Black, C. B. Murray, R. L. Sandstrom, S. H. Sun, *Science* **2000**, *290*, 1131–1134.
[9] a) C. P. Collier, T. Vossmeyer, J. R. Heath, *Annu. Rev. Phys. Chem.* **1998**, *49*, 371–404; b) C. B. Murray, C. R. Kagan, M. G. Bawendi, *Annu. Rev. Mater. Sci.* **2000**, *30*, 545–610.
[10] a) D. V. Talapin, E. V. Shevchenko, A. Kornowski, N. Gaponik, M. Haase, A. L. Rogach, H. Weller, *Adv. Mater.* **2001**, *13*, 1868–1871; b) E. V. Shevchenko, D. V. Talapin, A. L. Rogach, A. Kornowski, M. Haase, H. Weller, *J. Am. Chem. Soc.* **2002**, *124*, 11480–11485.
[11] a) F. X. Redl, K. S. Cho, C. B. Murray, S. O'Brien, *Nature* **2003**, *423*, 968–971; b) E. V. Shevchenko, D. V. Talapin, N. A. Kotov, S. O'Brien, C. B. Murray, *Nature* **2006**, *439*, 55–59.
[12] a) A. Courty, A. Mermet, P. A. Albouy, E. Duval, M. P. Pileni, *Nat. Mater.* **2005**, *4*, 395–398; b) H. F. Zhang, I. Hussain, M. Brust, M. F. Butler, S. P. Rannard, A. I. Cooper, *Nat. Mater.* **2005**, *4*, 787–793.
[13] a) J. J. Urban, D. V. Talapin, E. V. Shevchenko, C. B. Murray, *J. Am. Chem. Soc.* **2006**, *128*, 3248–3255; b) J. J. Urban, D. V. Talapin, E. V. Shevchenko, C. R. Kagan, C. B. Murray, *Nat. Mater.* **2007**, *6*, 115–121.
[14] A. M. Kalsin, M. Fialkowski, M. Paszewski, S. K. Smoukov, K. J. M. Bishop, B. A. Grzybowski, *Science* **2006**, *312*, 420–424.
[15] a) A. M. Kalsin, B. Kowalczyk, S. K. Smoukov, R. Klajn, B. A. Grzybowski, *J. Am. Chem. Soc.* **2006**, *128*, 15046–15047; b) N. Tomioka, D. Takasu, T. Takahashi, T. Aida, *Angew. Chem.* **1998**, *110*, 1611–1614; *Angew. Chem. Int. Ed.* **1998**, *37*, 1531–1534.
[16] X. G. Peng, *Adv. Mater.* **2003**, *15*, 459–463.
[17] a) A. Tao, P. Sinsermsuksakul, P. D. Yang, *Angew. Chem.* **2006**, *118*, 4713–4717; *Angew. Chem. Int. Ed.* **2006**, *45*, 4597–4601; b) M. J. Siegfried, K. S. Choi, *J. Am. Chem. Soc.* **2006**, *128*, 10356–10357; c) J. Y. Chen, J. M. McLellan, A. Siekkinen, Y. J. Xiong, Z. Y. Li, Y. N. Xia, *J. Am. Chem. Soc.* **2006**, *128*, 14776—14777; d) D. Seo, J. C. Park, H. Song, *J. Am. Chem. Soc.* **2006**, *128*, 14863–14870.
[18] Y. B. Chen, L. Chen, L. M. Wu, *Inorg. Chem.* **2005**, *44*, 9817–9822.
[19] Z. L. Wang, *J. Phys. Chem. B* **2000**, *104*, 1153–1175.

